



Electro-coagulation coupled Electro-floatation process: Feasible choice in Doxycycline removal from Pharmaceutical effluents

S. Zaidi, T. Chaabane, V. Sivasankar, A. Darchen, R. Maachi, T. A. M
Msagati

► To cite this version:

S. Zaidi, T. Chaabane, V. Sivasankar, A. Darchen, R. Maachi, et al.. Electro-coagulation coupled Electro-floatation process: Feasible choice in Doxycycline removal from Pharmaceutical effluents. Arabian Journal of Chemistry, 2019, 12 (8), pp.2798-2809. 10.1016/j.arabjc.2015.06.009 . hal-01165431

HAL Id: hal-01165431

<https://univ-rennes.hal.science/hal-01165431>

Submitted on 29 Jun 2015

HAL is a multi-disciplinary open access archive for the deposit and dissemination of scientific research documents, whether they are published or not. The documents may come from teaching and research institutions in France or abroad, or from public or private research centers.

L'archive ouverte pluridisciplinaire **HAL**, est destinée au dépôt et à la diffusion de documents scientifiques de niveau recherche, publiés ou non, émanant des établissements d'enseignement et de recherche français ou étrangers, des laboratoires publics ou privés.



Distributed under a Creative Commons Attribution - NonCommercial - NoDerivatives 4.0 International License



King Saud University

Arabian Journal of Chemistry

www.ksu.edu.sa
www.sciencedirect.com



ORIGINAL ARTICLE

Electro-coagulation coupled electro-flotation process: Feasible choice in doxycycline removal from pharmaceutical effluents

S. Zaidi ^a, T. Chaabane ^{a,*}, V. Sivasankar ^b, A. Darchen ^c, R. Maachi ^a,
T.A.M. Msagati ^d

^a University of Sciences and Technology Houari Boumediene, Faculty of Mechanical and Process Engineering/Environmental Department, BP 32, El-Alia 16111, Bab Ezzouar, Algiers, Algeria

^b P.G. and Research Department of Chemistry, Pachaiyappa's College, Chennai 600 030, Tamil Nadu, India

^c UMR CNRS n°6226 Institut des Sciences Chimiques de Rennes, ENSCR, 11, Allée de Beaulieu, CS 50837, 35708 Rennes Cedex 7, France

^d University of South Africa, College of Science Engineering and Technology, UNISA Science Campus, 1709 Roodepoort, Johannesburg, South Africa

Received 6 April 2015; accepted 6 June 2015

KEYWORDS

Electro-coagulation–flootation;
Aluminum electrodes;
Doxycycline hydicate

Abstract Electrochemical treatment involving a coupled coagulation and floatation was performed in the removal of doxycycline hydicate (DCH) from aqueous solutions. All the experiments were carried out in an electrochemical reactor of 1.5 L which contained aluminum electrodes as cathode and anode. The removal of doxycycline hydicate (DCH) species by EC/EF was determined as a function of electrolysis time, pH, current intensity, flow rate and DCH concentration. From the observed results, it was corroborated that the DCH removal through the EC/EF process was excellent. The effective contribution from initial pH (7.03) and current intensity (5.39 mA cm^{-2}) was very much remarkable and well apparent from flocs of good buoyancy. The removal of DCH was inversely proportional to spacing between electrodes (SBE) and circulating flow rate in the presence of the supporting NaCl electrolyte of 1 g L^{-1} . It was also highly promoted by the addition of NaCl in comparison with NaNO₃ and KCl to the electrolytic system. The compliance of four kinetic models was verified with DCH removal system. The free energy values from DKR model suggested the nature of bonding by chemical forces. Characterization by FTIR, SEM and XRD interpreted the assignments of various functional groups, surface morphology and crystalline

* Corresponding author. Tel.: +213 21247169.

E-mail address: tfkchaabane@yahoo.fr (T. Chaabane).

Peer review under responsibility of King Saud University.



Production and hosting by Elsevier

incorporated amorphous nature, respectively of electro-generated flocs. The current efficiency and specific electrical energy consumption at optimized conditions of the EC/EF system were calculated. © 2015 The Authors. Production and hosting by Elsevier B.V. on behalf of King Saud University. This is an open access article under the CC BY-NC-ND license (<http://creativecommons.org/licenses/by-nc-nd/4.0/>).

1. Introduction

In the recent years, the use of pharmaceuticals is of great concern among the researchers (Zhang et al., 2009) due to their environmental risks and treatments across the world. Chang et al. (2009) reported that the use of antibiotics and growth hormones affects the quality of surface and groundwater. Tetracycline has been the second reported antibiotic in its production and usage throughout the world (Wan et al., 2010) which affects the soil (O'Connor and Aga, 2007), surface water and groundwater (Tsai et al., 2010). Reports based on United States Pharmacopeia (USP) Convention (1997) revealed that tetracycline causes a permanent discoloration of teeth, enamel hypoplasia and inhibition of skeletal growth in the fetus, infants and children up to 8 years of age. Doxycycline (semi-synthetic form of tetracycline) is an effective antibiotic against a broad range of Gram-positive, Gram-negative bacteria and Rickettsia. Due to its highly soluble nature, doxycycline exhibits high residual toxicity in surface and groundwater. According to the European Directive 1907/2006/EC, Article 31 of safety data sheet, doxycycline is not allowed to enter sewers and surface or groundwater (Safety Data Sheet, 2014). As pharmaceuticals, even at very low concentrations can cause serious environmental damages, it is of great exigency to develop some efficient and cost-effective treatment technologies to remove such compounds. Okuda et al. (2008) achieved about 99% removal of 66 pharmaceuticals through ozone treatment coupled with coagulation and sand filtration. Choi et al. (2008) reported that the utilization of Granular Activated Carbon (GAC) from coal and coconut based carbons for the removal of tetracycline compounds could even yield more than 90% removal efficiency. Various techniques such as ozonation (Khan et al., 2010), Photo-Fenton process (Bautitz and Nogueira, 2007), photo electro-catalytic degradation (Liu et al., 2009), ion exchange (Wang et al., 2008) and adsorption (Reyes et al., 2006) have been chosen for the removal of tetracycline from water. Among the treatment processes, electro-coagulation has been reported to successfully treat wastewater containing oil (Chen et al., 2000), suspended particles (Larue et al., 2003), arsenic (Kumar et al., 2004), surfactants (Ge et al., 2004), chromium ions (Gao et al., 2005), dyes (Zaroual et al., 2006), potato chips manufacturing wastewater (Kobya et al., 2006), textile effluent (Zaroual et al., 2006), fluoride (Khatibikamal et al., 2010), laundry wastewater (Janpoor et al., 2011), municipal wastewater (Al-Shannag et al., 2013), baker's yeast wastewater (Al-Shannag et al., 2014), Strontium (Kamaraj et al., 2013) and heavy metal ions (Al-Shannag et al., 2015). Electro-coagulation (Holt et al., 2005) is an electrochemical technology of treating polluted water at the expense of sacrificial anodes at an optimized potential. Consequently, active coagulant precursors are formed. It is a process where multifarious mechanisms operate synergistically to remove the pollutants in wastewaters. It offers the possibility of anodic oxidation and in situ-

generation of active adsorbents (such as hydroxides of aluminum and iron). At the same time, cathodic reactions also occur, which led to the evolution of hydrogen gas causing floatation of the absorbents called electro-flootation. The electro-flootation process serves to the physical separation of solids and liquids by facilitating the pollutants to float on the surface of water body through the electrochemically generated hydrogen and oxygen during the electrolysis of water (Kotti et al., 2009).

Keeping in mind the above concerns, the present study was focused on the electro-coagulation coupled electro-flootation removal of doxycycline hydiate. The removal efficiency of doxycycline hydiate as a function of other system variables such as pH, current density, spacing between electrodes (SBE), DCH concentration, circulating flow rate, and supporting electrolytes was also studied and discussed.

2. Materials and methods

All the chemicals and reagents used in the study are all of analar grade. Doxycycline hydiate [4S,4aR,5S,5aR,6R,12aR-4-(di methylamino)-1,5,10,11,12a -pentahydroxy-6-methyl-3,12-dioxo-4a,5,5a,6-tetrahydro-4H-tetracene-2-carboxamidehydronchloride] was supplied by Sigma-Aldrich, Germany, and the structural formula is shown in Fig. 1. Stock solutions were prepared by dissolving an appropriate quantity of doxycycline hydiate in distilled water.

The experimental setup is as follows:

A coupled EC/EF system in a closed reactor through continuous mode was set up. The reactor capacity with the volume of 1.5 L was built at a laboratory scale as shown in Fig. 2.

In this electro-coagulation coupled electro-flootation (EC/EF) study, aluminum cathode and aluminum anode (11.9 cm × 4.7 cm × 0.4 cm) were designed to achieve the electro-coagulation process. The electro-flootation process was achieved using stainless steel anode and graphite cathode in 11.0 cm × 4.7 cm × 1.0 cm dimensions. The electrodes were connected to a digital DC supply (2303 GPS-type) with voltage

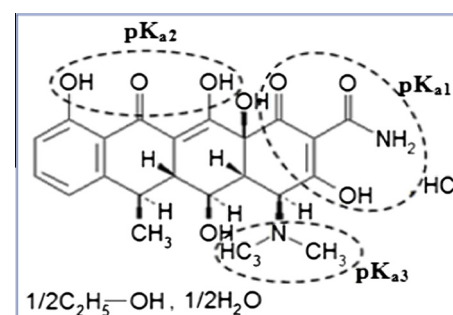


Figure 1 Chemical structure of doxycycline.

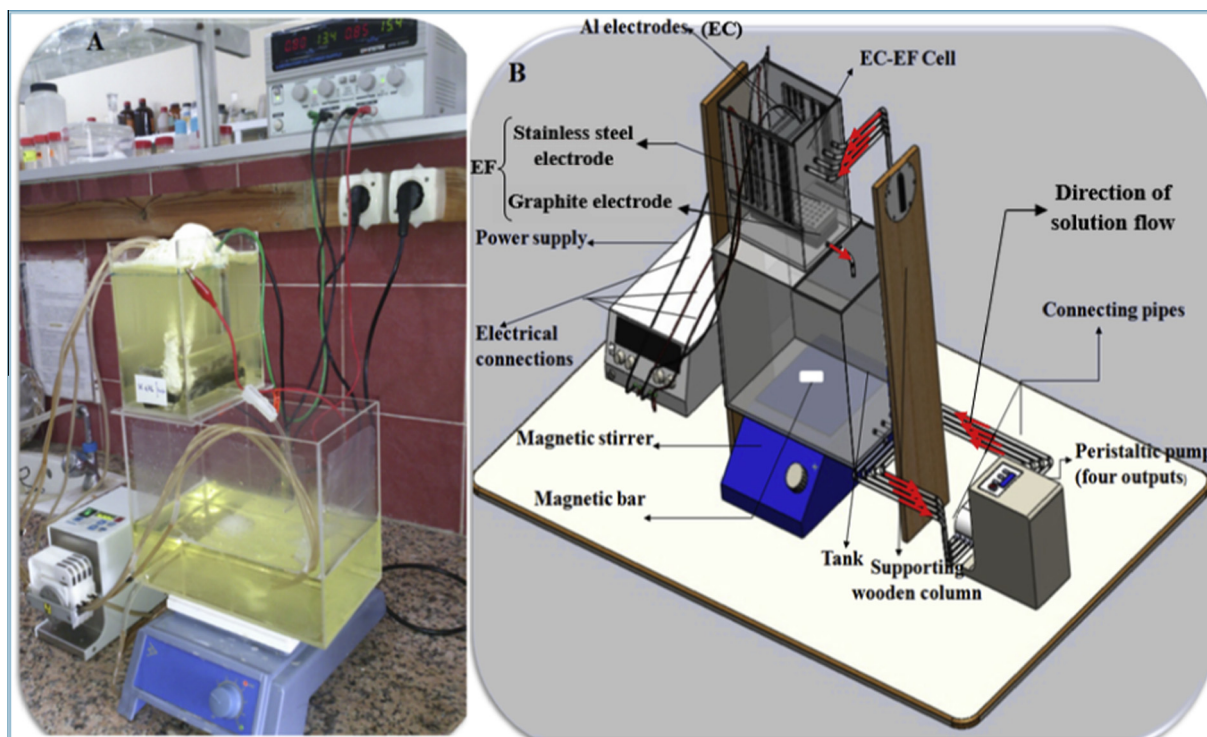


Figure 2 Prototype model of EC/EF cell (A) and schematic experimental setup of EC/EF cell (B).

and current range of 0–32 V and 0–4 A respectively. A digital ammeter and voltmeter were used to regulate the current and voltage. After each run of experiments, the used aluminum electrodes were rubbed with glass paper followed by immersion in NaOH solution of 0.1 M for 10 min. These electrodes were then rinsed with distilled water and dried at 105 °C for 10 min to remove surface impurities before re-use. The percentage removal of doxycycline hydulate as a function of time (*t*), pH, current density (*i*), spacing between electrodes (*d*), electrolyte type, circulating flow rate (*Q*) and initial concentration of DCH was determined by the following equation:

$$R (\%) = \left[\frac{C_0 - C_t}{C_0} \right] \times 100 \quad (1)$$

where C_0 is the initial DCH concentration and C_t is the remaining DCH concentration that was measured over time.

The residual doxycycline hydulate (DCH) concentration was determined by UV–Visible spectrophotometer (Shimadzu UV-1800, Japan) at a wavelength of 350 nm. Parameters such as pH and electrical conductivity measurements were respectively carried out by Sartorius checker pH meter (Sartorius Professional meter, PP-15, Germany) and HANNA bench conductivity (HANNA instruments, EC 214, Italy). An ISMATEC (ISM 834C) peristaltic pump equipped with four channels is provided with Tygon® tubes of 0.8 mm internal diameter. The recovered solid after treatment was dried at 110 °C for about 5 h and then characterized by FTIR, SEM and XRD instrumental studies using FTIR spectrometer PerkinElmer (Version 10.03.06), X’Pert PRO X-ray diffractometer (PANalytical) and scanning electron microscope (JEOL, JSM-6360), respectively. Models on adsorption kinetics and isotherms are detailed in Table 1.

3. Results and discussion

3.1. Effect of current density and time of electrolysis

In all electrochemical reactions, the reaction rate is controlled by current density and time of electrolysis which determine the coagulant production rate and the total production of coagulant respectively. The percentage removal of DCH as a function of time at different current densities (3.59 mA cm⁻²–14.39 mA cm⁻²) is shown in Fig. 3A. It can be illustrated that the current density of 5.39 mA cm⁻² was the optimum current density based on the maximum DCH removal and consumed time for electrolysis. The removal of DCH was almost 90% after 80 min. The residual DCH concentration was in the range 1.60–5.18 mg L⁻¹. Although the DCH removal was remarkable with the residual DCH concentration of 0.53 mg L⁻¹ at 14.39 mA cm⁻², the consumption of current was 2.7 times higher with respect to the optimized current (current density = 5.39 mA cm⁻²) which leaves the residual DCH concentration of 0.76 mg L⁻¹.

The rate of DCH removal was directly proportional to current density because of the increased production of the coagulant (Al³⁺ ions) on the anode. As a result of increased flocs generation rate, the DCH removal efficiency was enhanced. In other words, the higher the current density, the greater will be the generated flocs to trap the DCH molecules from the aqueous solution. After the time of electrolysis in the range of 50–60 min, the residual DCH concentration was very low. The rate of its sorption onto the generated flocs at constant rate tends to decrease for a particular current density.

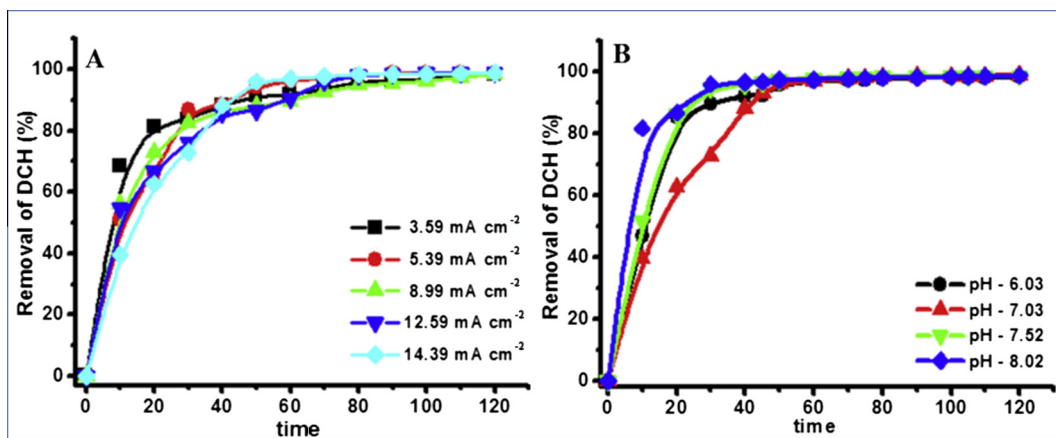
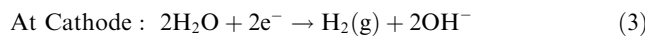


Figure 3 Removal of DCH as a function of current density (A) and pH of the solution (B). Conditions: (A) pH = 7, [DCH] = 100 mg L⁻¹, Q = 52 L min⁻¹, d = 1 cm, conductivity = 1.78 mS cm⁻²; (B) [DCH] = 100 mg L⁻¹, CD = 5.39 mA cm⁻², Q = 52 mL min⁻¹, d = 1 cm, conductivity = 1.78 mS cm⁻¹.

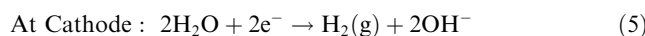
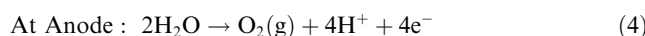
3.2. Effect of pH

The pH of any electrolyte drives the fate of electro-coagulation process (Yavuz et al., 2011). The pH of the electrolytic medium increases during the flocculation–sorption phase and gets stabilized in the pH range 7.52–7.91 for various initial DCH concentrations at an initial pH of 7.0 as reported by Yavuz et al. (2011). The associated increase in pH may be corroborated due to the electrolysis of water leading to hydrogen evolution and OH⁻ production (Malakootian et al., 2010). The relative stability of pH after the process could be ascertained due to the formation of Al(OH)₃ flocs with less solubility between the pH values of 6 and 8 (Emamjomeh and Sivakumar, 2009). The effect of pH on DCH removal is shown in Fig. 3B. The removal of DCH at different pH values of 6.03, 7.04, 7.52 and 8.02 was conducted with the initial DCH concentration of 100 mg L⁻¹. The increased precipitation at higher pH leading to the generation of greater flocs enhances the DCH removal efficiency. The removal of DCH was achievable between 98.5% and 99.4% in the pH range 6.03–8.02. Similar observation was experienced in the study of boron removal by Ezechi et al. (2014).

The main reactions that take place during electro-coagulation at the two electrodes are as follows:



while the chemical reactions taking place during electro-flotation are given as follows:



Under acidic condition (pH < 3.3) due to protonation, the cationic form of DCH (+00) develops the electrostatic repulsion with predominant cationic monomers of Al³⁺ and Al(OH)²⁺ and lessens the removal efficiency of DCH (Ouaissa et al., 2014). The possibility of DCH speciation at various pH values (Zhang et al., 2011) as zwitterion (± 0)

was due to the loss of proton from the phenolic diketone moiety. On the other hand, the pH between 6.03 and 8.02 generates Al³⁺ and OH⁻ ions to form various monomers such as Al(OH)⁺, Al(OH)²⁺ and other polymeric species such as Al₆(OH)³⁺, Al₇(OH)⁴⁺, Al₁₃(OH)⁵⁺ which were finally converted into the insoluble amorphous Al(OH)_{3(s)} through complex polymerization/precipitation kinetics (Merzouk et al., 2009). The formation of Al(OH)_{3(s)} is therefore optimal in the 4–9 pH range. In addition, the cathode (Al) may be chemically attacked by OH⁻ ions generated together with H₂ at high pH values as



However, the pH affects also the bubble size (Glembotskii et al., 1975). Typical bubble sizes in electro-coagulation always fall in the range of 20–70 µm (Adhoum et al., 2004). They are far smaller than those observed in conventional air-assisted floatation, which provides both sufficient surface area for gas–liquid–solid interfaces and mixing efficiency to favor the aggregation of tiny destabilized particles. Hydrogen bubbles, which usually obey to a lognormal size distribution, are also known to be the smallest at about neutral pH (Fukui and Yuu, 1985). The best removal of DCH could be accomplished by charge neutralization and sorption in the presence of the constituent monomers and polymers. The acquired surface positive sites with large surface area on the amorphous structure of hydrolyzed Al(OH)₃ make the viability of sorption with the macromolecular organic DCH anions rather existing as a free hydrated metal ion (Zhou et al., 2008). It is also envisaged that the DCH at basic conditions prevails as either a monovalent or a divalent anion due to deprotonation of tricarbonyl system and phenolic diketone moiety. As a consequence, high removal of DCH may be associated, due to the attractive force between the positive aluminum and negative DCH ions, and hence the sorption of the latter onto Al(OH)₃. These active flocs facilitate the rapid sorption of soluble DCH compound being entrapped by the colloidal particles and ultimately get separated from the aqueous medium by sedimentation or hydrogen floatation (Ghernaout et al., 2009). The surface complexes of zwitterionic species were previously suggested by Figueroa et al. (2004).

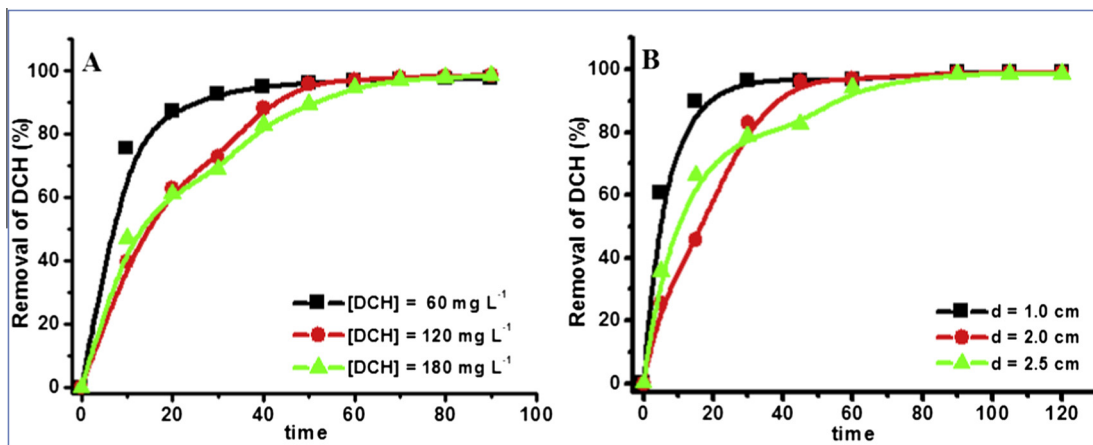


Figure 4 Removal of DCH as a function of initial DCH concentration (A) and spacing between electrodes (B). Conditions: (A) pH = 7, CD = 5.39 mA cm⁻², Q = 52 mL min⁻¹, d = 1 cm, conductivity = 1.78 mS cm⁻¹; (B) pH = 7, [DCH] = 100 mg L⁻¹, CD = 5.39 mA cm⁻², Q = 52 mL min⁻¹, conductivity = 1.78 mS cm⁻¹.

3.3. Effect of spacing between electrodes (SBE)

The spacing between electrodes and effective surface area depends on the construction of the electrode assembly. The variation in voltage drop (η_{IR}) is governed by the following equation (Ghosh et al., 2008a):

$$\eta_{IR} = I \cdot d / S \cdot k \quad (7)$$

where I = current (A), d = spacing between two electrodes (cm), S = active anode surface (cm²), and k = specific conductivity (10³ mS cm⁻¹) with constant anodic surface area and conductivity. The increase in the electrode spacing increases the resistance between them with a decrease in the electric current. The increased SBE leads to lessen the interaction of ions with hydroxide polymers. The DCH removal as a function of SBE was studied for 1 cm, 2 cm and 2.5 cm with an initial DCH concentration of 100 mg L⁻¹ as shown in Fig. 4B. The removal efficiency was around 96% at the end of 30 min, 45 min and 60 min respectively. The results substantiate that the DCH removal was inversely proportional to the magnitude of SBE. This observation is probably based on the voltage and hence the required power consumption is low for the movement of ions (Vasudevan et al., 2013). It may also be suggested that the increase in the local concentration of DCH ions with monomeric and polymeric hydroxo-cationic species generated within a smaller space which lead to an increase in the electrostatic interaction and hence the removal of dissolved DCH ions becomes facilitated (Mansour et al., 2012). It is also accounted that the shorter travel path reduces the resistance during the ionic motion and thus the remaining experiments were conducted with an SBE distance of 1 cm.

3.4. Effect of initial DCH concentration

The initial concentration provides an important driving force to overcome all mass transfer resistance of solutes between the aqueous and the solid phase (Ji et al., 2009). The removal efficiency of DCH as a function of initial DCH concentration at 5.39 mA cm⁻² is shown in Fig. 4A. The percentage of DCH

removal was decreased with respect to the increase in the initial concentration and could easily be distinguishable up to 50 min. But after 50 min, the residual DCH concentration falls between 2.3 mg L⁻¹ and 2.6 mg L⁻¹. As per Faraday's law, at a constant current density, the generated aluminum flocs for a particular time remain constant for various DCH concentrations (60–180 mg L⁻¹). But the requirement of aluminum flocs will be greater for the higher DCH concentration and hence becomes insufficient to capture the extra organic DCH species. Evidently single, smooth and continuous graphical curves leading to saturation which suggests the monolayer coverage of DCH on the surface of Al(OH)₃ were reported (Lakshmi et al., 2013).

3.5. Effect of supporting electrolytes

In order to increase the conductivity of wastewater due to resistance between the electrodes, the addition of sodium chloride is suggested during electro-coagulation process.

Researchers used sodium chloride to increase the conductivity of the solution; nevertheless, sodium nitrate and sodium sulfate were also used as electrolytes (Aber et al., 2009). On increasing the salt concentration, the power consumption of electrolytic cells is reduced due to the reduction in cell voltage at constant current density (Kashefalias et al., 2006). Although the type of electrolyte has no effect in favor of the removal efficiency, it provides the pronounced effect on cell voltage and current consumption during the EC process. It is also reported that at high anode potential, direct oxidation of organic compounds or H₂O may also take place (Ge et al., 2004). The influence of sodium chloride was remarkable in facilitating the removal of DCH, whereas the influence of sodium nitrate and potassium chlorides was alike and their effect on the removal of DCH was almost closer to each other. The intertwined curves shown in Fig. 5B illustrate that no appreciable influence was observed due to the addition of sodium nitrate and potassium chlorides. The conductivity of the solution remains practically constant during the treatment as shown in Fig. 5C. The average electrical conductivity of DCH

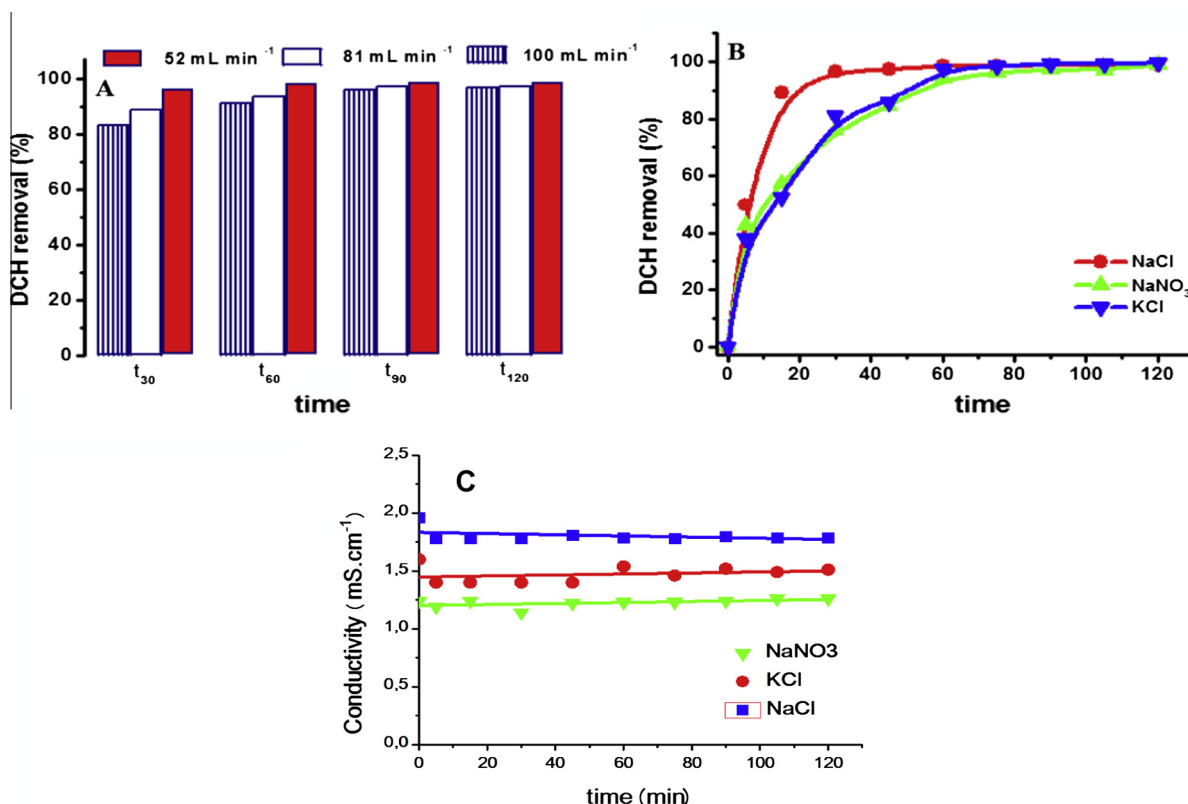


Figure 5 Removal of DCH as a function of circulating flow rate (A), electrolyte interference (B) and evolution of conductivity as a function of time for each electrolyte (C). *Conditions:* (A) pH = 7, CD = 5.39 mA cm⁻², [DCH] = 100 mg L⁻¹, d = 1 cm, conductivity = 1.78 mS cm⁻¹; (B) pH = 7, [DCH] = 100 mg L⁻¹, CD = 5.39 mA cm⁻², Q = 52 mL min⁻¹, d = 1 cm; (C) pH = 7, [DCH] = 100 mg L⁻¹, CD = 5.39 mA cm⁻², d = 1 cm, Q = 52 mL min⁻¹.

electrolyte in the presence of sodium chloride was recorded to be 1.78 mS cm⁻¹. The electrical conductivity of the DCH electrolyte in the presence of KCl and NaNO₃ was recorded as 1.45 mS cm⁻¹ and 1.22 mS cm⁻¹ respectively. Hence it is apparent that high conductivity of the EC system due to NaCl enables the DCH removal of about 90% at the end of 30 min but for the other salts (KCl and NaNO₃) the same percentage of removal could be achieved after 60 min. From the above observations, it is quite understood that half of the power is expendable to achieve 90% removal of DCH in the presence of sodium chloride as compared to the other potassium chloride and sodium nitrate as supporting electrolytes.

3.6. Effect of circulation flow rate

The effect of the circulating flow rate of 52 mL min⁻¹, 82 mL min⁻¹ and 100 mL min⁻¹ on the removal of DCH at a concentration of 100 mg L⁻¹ is shown in Fig. 5A. In general, the performance of the EC column toward removal of desired solute is inversely proportional to the flow rate.

The percentage of DCH removal increased with respect to the decrease in the flow rate. High removal of DCH can be attributed to the increased residence time of DCH molecules inside the EC column due to the restricted flow rate and hence long reaction time between DCH species and the aluminum flocs (Lin and Peng, 1996). Contrarily, low residence time due to the short stay of DCH species inside the EC column facilitates insufficient interaction between DCH species and

the aluminum flocs (Bratby, 2006). It is reported that (Al-Shannag et al., 2012) the increasing circulating flow rate will generate high mixing levels within the EC unit that could facilitate the transport process of colloidal pollutants to be adsorbed onto the active sites of coagulants. Conversely, at very high circulating flow rate, the coagulants would dissociate and lead to the hindrance of the sorption process with decreased removal efficiency. From the observed results, an increased difference of 12.75% was observed from the flow rate of 52–100 mL min⁻¹ after the time of 30 min. But the margin of increased difference was halved (6.82%) after 60 min. On proceeding to 90 min and 120 min, the differential margin was about 2.21% and 1.82% respectively. A longer electrolysis time of about 120 min was needed to achieve the maximum DCH removal for the high flow rate of 100 mL min⁻¹.

3.7. Kinetic models

The study on adsorption kinetics is significant because it provides valuable insight into the reaction pathway and the corresponding sorption mechanism. The sorption mechanism depends on the physical and chemical characteristics of the adsorbent and also on the mass-transfer process. The dynamics of DCH sorption onto Al(OH)₃ at an optimized pH (7.02) with respect to different spacing between electrodes, initial DCH concentrations, supporting electrolytes and circulating flow rate was validated using kinetic models such as pseudo-first-order, pseudo-second-order, intra-particle diffusion and

Table 1 Kinetic and isotherm model equations and relevant details.

Model	Equation	Plotting parameters as		Notations and units	Reference	Equation number
		X	Y			
1. Pseudo-first-order	$\ln(q_e - q_t) = \ln q_e - k_1 t$	time (t)	$\ln(q_e - q_t)$	$k_1 \rightarrow$ Pseudo-first-order rate constant in min^{-1}	Lagergren (1898)	Eq. (8)
2. Pseudo-second-order	$\frac{dq}{dt} = k_2 (q_e - q_t)^2$ $t/q_t = 1/k_2 q_e^2 + (1/q_e)t$	time (t)	t/q_t	$k_2 \rightarrow$ Pseudo-second-order rate constant in $\text{g mg}^{-1} \text{min}^{-1}$; $h (=k_2 q_e^2) \rightarrow$ initial sorption rate in $\text{mg g}^{-1} \text{min}^{-1}$	Ho (2006)	Eq. (9)
3. Intra-particle diffusion	$q_t = k_i t^{1/2} + C$	time $t^{1/2}$ or $(t)^{1/2}$	q_t	$k_i \rightarrow$ intraparticle rate constant in $\text{mg g}^{-1} \text{min}^{-0.5}$; $C \rightarrow$ thickness of the boundary layer in mg g^{-1}	Weber and Morris (1963)	Eq. (11)
4. Elovich	$q_t = (1/B) \ln AB + (1/B) \ln t$	$\ln t$	q_t	$A \rightarrow$ initial adsorption rate in $\text{mg g}^{-1} \text{min}^{-1}$; $B \rightarrow$ constant of desorption in g mg^{-1}	Aharoni and Tompkins (1970)	Eq. (12)
5. DKR	$\ln q_e = \ln q_m - B \varepsilon^2$ $E = (2B)^{-1/2}$ $\varepsilon = RT \ln(1 + 1/C_e)$	ε^2	$\ln q_e$	$q_e \rightarrow$ amount of DCH adsorbed per unit weight of adsorbent (mg g^{-1}); $q_m \rightarrow$ monolayer adsorption (mg g^{-1}) capacity (mmol g^{-1}) β -constant related to adsorption energy ($\text{mol}^2 (\text{kJ})^{-1}$)	Dubinin and Radushkevich (1947)	Eq. (13) Eq. (14) Eq. (15)

In the above models, q_t and q_e are the amount of DCH adsorbed at time t and equilibrium respectively in mg g^{-1} .

Table 2 Validity of kinetic models with the EC based removal of doxycycline hyolate.

	Spacing between electrodes (cm)			DCH concentration (mg L^{-1})			Electrolyte (g L^{-1})			Circulating flow rate (mL min^{-1})		
	1	2	2.5	60	120	180	NaNO ₃	KCl	NaCl	52	81	100
<i>Pseudo-first-order</i>												
q_e	34.30	111.11	131.60	225.61	225.20	26.22	29.62	61.63	93.42	62.55	76.32	22.49
$k_1 \times 10^{-2}$	6.011	7.321	6.531	6.322	8.723	7.722	6.114	2.743	5.642	4.020	5.520	6.020
R^2	0.941	0.982	0.958	0.961	0.967	0.994	0.933	0.906	0.965	0.944	0.873	0.950
<i>Pseudo-second-order</i>												
q_e	109.83	125.02	111.11	52.63	125.02	200.04	110.72	109.78	109.88	108.69	109.89	111.12
h	43.48	7.63	10.20	17.24	6.71	10.05	10.53	23.81	9.43	12.50	19.61	43.48
$k_2 \times 10^{-4}$	0.352	4.881	8.261	0.622	4.293	2.514	8.523	0.193	7.642	0.106	0.162	0.352
R^2	0.999	0.987	0.998	0.999	0.989	0.994	0.997	0.996	0.995	0.999	0.999	0.999
<i>Intra-particle diffusion</i>												
k_i	3.240	8.158	6.573	1.525	9.223	12.880	5.060	6.128	6.530	3.871	2.721	2.020
C	69.12	22.56	34.96	36.06	20.87	35.43	54.46	35.79	37.04	58.96	71.65	79.96
R^2	0.598	0.78	0.863	0.783	0.874	0.949	0.524	0.927	0.873	0.912	0.913	0.553
<i>Elovich</i>												
A	182.47	1.85	1.76	519.20	1.93	1.55	5.79	2.42	2.28	13.84	328.14	5062.40
B	0.094	0.039	0.051	0.208	0.035	0.026	0.059	0.056	0.052	0.072	0.103	0.128
R^2	0.790	0.907	0.970	0.898	0.950	0.976	0.722	0.983	0.923	0.970	0.970	0.688

Elovich models. The figured parameters of the kinetic models are represented in Table 2.

Based on pseudo-first-order and pseudo-second-order models, it is possible to elucidate the mechanism of adsorption and potential rate controlling steps (Chutia et al., 2009) of DCH sorption onto Al(OH)₃ flocs.

Pseudo-first-order model is a simple adsorption kinetic model (Eq. (8)), suggested by Lagergren (1898) and further referred by Ho et al. (1996), which is unable to apply throughout the range of tested contact time. The kinetic parameters q_e and k_1 were calculated from the intercept and slope respectively using Eq. (8) and are shown in Table 2. The regression

values (R^2) inferred that the DCH sorption complies fairly well with the pseudo-first-order model.

According to pseudo-second-order kinetics (Eqs. (9) and (10)), the rate of adsorption is directly proportional to the number of active sites on the adsorbent surface. The kinetic parameters calculated from the pseudo-second-order equation (Eq. (10)) were q_e , k_2 and h from the slope and intercept values ($q_e = 1/\text{slope}$; $k_2 = \text{slope}^2/\text{intercept}$; $h = 1/\text{intercept}$). The increase in the q_e value from 52.63 mg g^{-1} to 200.04 mg g^{-1} was recorded with respect to the DCH concentration. The R^2 values for all the variables (Table 2) were quite plausible and corroborate that the pseudo-second-order seems

appreciable with the DCH sorption kinetics. Based on the regression values, it may be ascertained that the pseudo-second-order was more validated than the pseudo-first-order model (Isa et al., 2014; Kamaraj and Vasudevan, 2015).

It is inferred from the Weber–Morris intra-particle diffusion plot (Eq. (11)) that the initial curved portion reflects the film or boundary layer diffusion effect and the subsequent linear portion (plateau) depicts the intra-particle diffusion effect. The graphical plots deviate from passing through the origin and this deviation may be caused due to the difference between the rate of mass transfer in the initial and final stages of DCH sorption and the complex mechanism. The mechanism of sorption thus involves the contribution of both the surface adsorption and intra-particle diffusion to the rate determining step. The thickness of boundary layer, determined from the intercept value C is inversely proportional to the external mass transfer. The value of C seems to be very sensitive with respect to the change in initial DCH concentration, SBE, supporting electrolyte and circulating flow rate. The regression values indicate the intra-particle diffusion model did not fit satisfactorily with the DCH sorption dynamics (Kamaraj et al., 2013).

Elovich model (Eq. (12)) is one among the useful kinetic models (Aharoni and Tompkins, 1970) and predicts the behavior of sorption over the whole range of variable studied. This fact strongly supports its validity and suggests that the adsorption is rate-determined by a chemisorptions step (Juang and Chen, 1997).

The value of $1/B$ gives about the number of available sites for sorption in the adsorbent. The magnitude of $1/B$ increased with respect to the increase in the initial concentration of DCH in several folds was established. On the contrary, the decrease in the available sites ($1/B$) was observed from 13.89 to 7.81 when the circulating flow rate was increased from 52 mL min^{-1} to 100 mL min^{-1} and becomes evident for the descending DCH removal efficiency. The calculated values of initial adsorption rate (A) and constant of desorption (B) with corresponding regression coefficients indicated that the Elovich model fits fairly well with the present system on DCH sorption onto Al(OH)_3 flocs (Kamaraj et al., 2013).

3.8. Isotherm model: Dubinin–Kaganer–Radushkevich (DKR) model

Dubinin–Kaganer–Radushkevich (DKR) isotherm is more general than Langmuir isotherm owing to its disagreement for a homogenous surface or a constant adsorption potential. Using DKR equation with reference to the present system, the constant β gives the free energy, E (kJ mol^{-1}) for the transfer of 1 mol of DCH ion from infinity to the surface of Al(OH)_3 flocs and can be computed using the relationship (Onyango et al., 2004) as shown in Eqs. (13)–(15). The magnitude of E is helpful in understanding the nature of DCH ion sorption. The recorded values of E with respect to the variation of DCH concentration and spacing between electrodes are $7.905 \text{ kJ mol}^{-1}$ and $15.813 \text{ kJ mol}^{-1}$ respectively. As the values are in the range of $8\text{--}16 \text{ kJ mol}^{-1}$, it may be suggested that the nature of bonding is governed by chemical forces (Swain et al., 2009). The present sorption system fits well with the DKR model and was supported by the R^2 values (Fig. 6) as reported by Kamaraj et al. (2013).

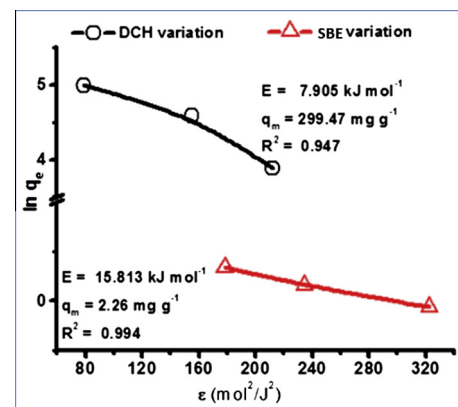


Figure 6 DKR model for DCH and SBE variations.

3.9. Characterization studies

The material after the EC/EF process was characterized by FTIR, SEM and XRD studies. The assignments of Fourier Transform IR study which occur at different frequencies are shown in Table 3 (Fig. 7B). The broadband appears between 3500 cm^{-1} and 3000 cm^{-1} with an assignment of 3307.56 cm^{-1} . This displacement was due to the displacement of OH band by overlapping of hydrogen bonds and the superimposition of NH band. The absence of $>\text{C=O}$ stretching frequency ($>\text{C=O}$ at 1715 cm^{-1} , $-\text{COOH}$ between 1700 and 1730 cm^{-1}) may be associated due to the newly formed bond between carbonyl oxygen and aluminum ions (as $>\text{C—O—Al}$).

The X-ray diffraction patterns (Fig. 7A) for DCH and DCH adsorbed Al(OH)_3 illustrate the amorphous and crystalline merged amorphous patterns respectively. The narrow diffraction peaks at 18.8° , 20.3° , 27.9° , 40.3° and 53.2° are assigned to bayerite (PDF No. 20-11). The retained amorphous pattern of DCH is perturbed with the overlapping crystalline pattern due to the DCH adsorbed polymorph, Al(OH)_3 . In support of the present study, it was reported that the formation of bayerite was predominant at near neutral pH ($\text{pH} \geq 7$) and higher pH values (Carrier et al., 2007). The amorphous or slightly crystalline nature of electro-generated aluminum hydroxides and oxo-hydroxides was remarkable because of the very slow crystallization process. Hence the reflections of

Table 3 FTIR assignments and associated stretching frequencies.

Organic function	Type of the bond	Theoretical values, cm^{-1}	Experimental values, cm^{-1}
Halogenated	$\gamma_{\text{C}-\text{Cl}}$	750–850	811.05
Alcohols	$\gamma_{\text{O}-\text{H}}$	3400	3307.56
	$\gamma_{\text{C}-\text{O}}$	1050	1062.22
	$\gamma_{\text{C}-\text{O}}$	1210–1320	1249.69
Oxides	$\gamma_{\text{C}-\text{O}}$	1070–1150	1168.45
Aromatics	$\gamma_{\sigma\text{C}-\text{C}}$ (deform)	1450–1600	1460.08
	$\gamma_{\sigma\text{C}-\text{H}}$	3020–3050	3307.56
Alkenes	$\gamma=\text{C}-\text{H}$	3020–3140	3307.56
	$\gamma_{\text{C}=\text{C}}$	1645	1599.37
Amines	$\gamma_{\text{N}-\text{H}}$	3300–3500	3307.56

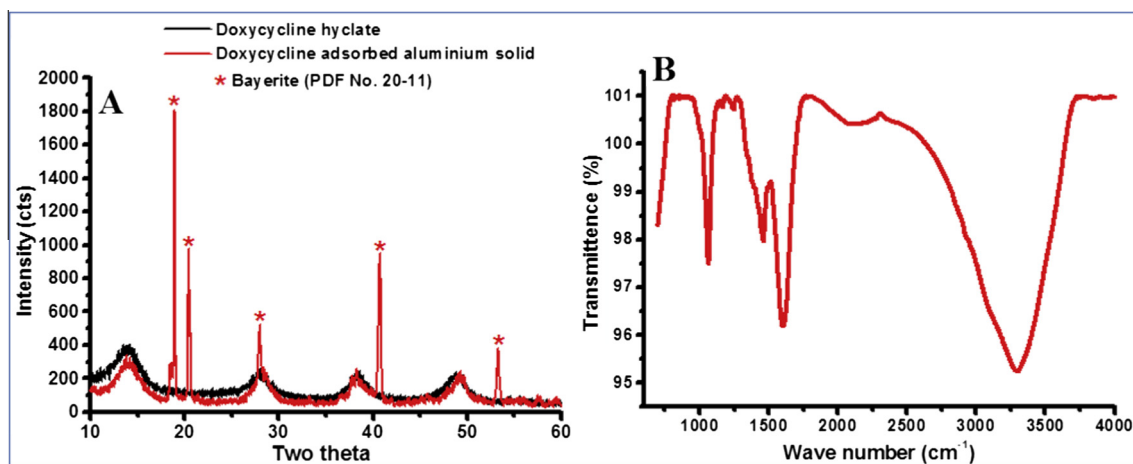


Figure 7 X-ray diffraction pattern (A) and FTIR of electro-generated coagulant with DCH (B).

Bragg showing very broad bumps with low intensity for the phases were analyzed at short distances (Drouiche et al., 2009).

The scanning electron micrograph (Fig. 8) shows that the aluminum floc-bound DCH material was at greater heterogeneity with irregular, sharp edged particles and exposing a rough surface. The precipitated grains constitute the distinguished geometries and make the formed aggregates with no well defined structural pattern.

3.10. Energy, electrodes and chemicals consumptions

Energy consumption and sacrificial electrodes are very important economical parameters. In this study, we used an average potential for EC and EF with a current density of 5.39 mA cm⁻². The electrical energy consumption of the process (EEC) was calculated using the following equation (Isa et al., 2014):

$$\text{EEC} = \text{EEC}_{\text{EC}} + \text{EEC}_{\text{EF}} = (IUt)/V \quad (16)$$

where EEC is the sum between the energy consumption of EC and EF (kW h m⁻³), I is current (A), U is voltage (V), t is time (h) and V is volume (L).

Current efficiency (φ) which depends on the anodic dissolution is calculated as follows (Ghosh et al., 2008b):

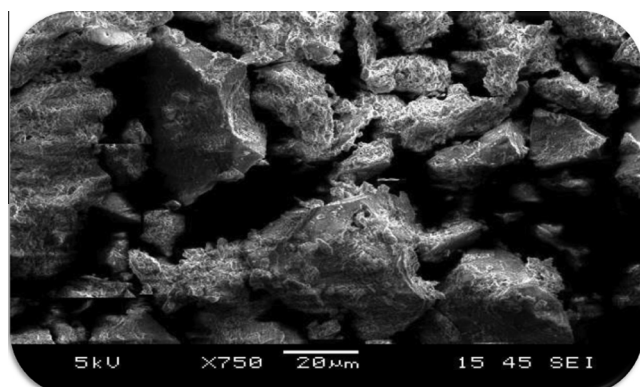


Figure 8 Scanning electron micrographs of electro-generated aluminum coagulant.

$$\varphi (\%) = \Delta M_{\text{exp}} / \Delta M_{\text{theo}} \times 100 \quad (17)$$

$$\Delta M_{\text{theo}} = MI t_{\text{EC}} / nF \text{ (Faraday's law)} \quad (18)$$

$$\Delta M_{\text{exp}} = m_{\text{Al}_i} - m_{\text{Al}_f} \quad (19)$$

where ΔM_{exp} and ΔM_{theo} are respectively experimental weight loss of aluminum electrodes (g) and theoretical amount of dissolved aluminum (g); M is molecular weight of aluminum (g mol⁻¹), n number of electron moles, F is Faraday constant ($F = 96,487 \text{ C mol}^{-1}$) and t_{EC} is time (s) of EC operation. As $\text{Al(OH)}_{3(s)}$ is supposed to be the formed species, the number of electron moles in dissolution reaction is equal to 3. Finally, m_{Al_i} and m_{Al_f} are respectively weights of the aluminum anode (g) before and after treatment. The experimental values are approximately equal to the theoretical values for the three electrolytes used as shown in Table 4.

Specific Electrical Energy Consumption (SEEC) is calculated as a function of aluminum electrodes weight consumption during EC in kW h per kg of Al (Nandi and Patel, 2014).

$$\text{SEEC} = (n \times F \times U) / (3600 \times M \times \varphi) \quad (20)$$

Table 5 represents the details of the current efficiency, amount of generated sludge and the consumption of specific electrical energy, electrode and electrolyte during the EC-EF process.

In supporting the obtained results, the consumption of electrical energy (C_{energy}) for NaNO_3 is 2.53 times higher than for NaCl . The amount of electrode consumed was intermediate for NaCl (61.8 g) when compared with KCl (60.1 g) and NaNO_3 (63.7 g). The sludge generation after the electrolysis process was two times higher for NaCl as compared to that of KCl . Hence it may be accounted that the influence of electric charge to generate more sludge was higher for NaCl than the other two supporting electrolytes. The specific electrical energy

Table 4 Operating parameters and amounts of dissolved aluminum.

Electrolyte used	UEC (V)	UEF (V)	ΔM_{exp} (g)	ΔM_{theo} (g)
NaNO_3	13.15	11.35	0.2547	0.2013
NaCl	4.25	5.45	0.2471	0.2013
KCl	4.30	5.70	0.2403	0.2013

Table 5 Details on the consumptions and sludge generations during EC-EF treatment.

Electrolyte used	φ (%)	SEEC (kW h/kg Al)	C_{energy} (ECC) (kW h/m ³)	$C_{\text{electrode}}$ (kg electrode/m ³)	$C_{\text{electrolyte}}$ (kg electrolyte/m ³)	C_{sludge} (kg (sludge/m ³)
NaNO ₃	126.5	30.97	3.675	0.0637	1.0	0.3319
NaCl	122.8	10.32	1.455	0.0618	1.0	0.2981
KCl	119.4	10.74	1.505	0.0601	1.0	0.1455

consumption (SEEC) for the supporting electrolytes is in the following order: NaNO₃ > KCl > NaCl. SEEC was observed about 3 times higher for NaNO₃ than NaCl and KCl during the process of EC. The difference in SEEC among the electrolytes may be attributed by the developed resistance between the electrodes with a particular electrolytic solution. In this case, the resistance developed was higher for NaNO₃ than KCl and NaCl electrolytic solutions. As a consequence of increased resistance, the voltage across the electrodes was increased. This behavior ultimately leads to increased total power consumption and SEEC for achieving the necessary current density to facilitate the EC process. The current efficiency (φ) of 119.4%, 122.8% and 126.5% was evaluated for the supporting electrolytes of NaCl, KCl and NaNO₃ respectively.

4. Concluding remarks

The electro-coagulation based removal of DCH was optimized at the pH of 7.03 which facilitated almost 90% removal after 80 min. The final pH of the electrolytic solutions was stabilized in the range of 7.52–7.91. DCH removal of about 96% was achievable with respect to the direct proportionality between spacing between electrodes and time of electrolysis. The supporting electrolyte contribution from NaCl was highly remarkable in facilitating the removal of DCH because of its highly conducting nature as compared to the other KCl and NaNO₃ electrolytes. The circulating flow-rate and removal efficiency were inversely related to each other based on the fact of residence time of DCH molecules. Among the kinetic models, pseudo-second-order model was with great compliance than pseudo-first-order model. DKR model suggested that the nature of bonding between DCH and aluminum flocs was governed by chemical forces. FTIR study corroborated the formation of new bonds between carbonyl oxygen (of DCH molecules) and aluminum ions (of flocs). X-ray diffraction study confirms that the formed aluminum flocs correspond to the bayerite pattern as shown by the corresponding peaks. The morphological pattern ascertained that the surface of the electro-generated solid was highly heterogeneous and irregular with precipitated grains. The present EC coupled EF treatment process may better be opted with the supporting electrolyte of NaCl because it requires less energy consumption. Nevertheless, an appropriate modification of the system needs to be explored to lessen the amount of sludge generation by the present EC-EF process.

Acknowledgments

In completing this modest contribution of research, I would like to thank the Heads of the collaborating educational institutes namely National College of Chemistry, Rennes top

(France), Research Department of Chemistry, Pachaiyappa's College, Chennai, India, and University of Sciences and Technology Houari Boumediene Algiers (Algeria) and P.G.

References

- Aber, S., Amani-Ghadim, A.R., Mirzajani, V., 2009. Removal of Cr(VI) from polluted solutions by electrocoagulation: modeling of experimental results using artificial neural network. *J. Hazard. Mater.* 171, 484–490.
- Adhoum, N., Monser, L., Bellakhal, N., Belgaid, J., 2004. Treatment of electroplating wastewater containing Cu²⁺, Zn²⁺ and Cr(VI) by electrocoagulation. *J. Hazard. Mater. B* 112, 207–213.
- Aharoni, C., Tompkins, F.C., 1970. Kinetics of adsorption and desorption and the Elovich equation. In: Eley, D.D., Pines, P., Weisz, P.B. (Eds.), . In: Advances in Catalysis and Related Subjects, vol. 21. Academic Press, New York.
- Al-Shannag, M., Lafi, W., Bani-Melhem, K., Gharagheer, F., Dhamat, O., 2012. Reduction of COD and TSS from paper industries wastewater using electro-coagulation and chemical coagulation. *Sep. Sci. Technol.* 47 (5), 700–708.
- Al-Shannag, M., Bani-Melhem, K., Al-Anber, Z., Al-Qodah, Z., 2013. Enhancement of COD-nutrients removals and filterability of secondary clarifier municipal wastewater influent using electrocoagulation technique. *Sep. Sci. Technol.* 48 (4), 673–680.
- Al-Shannag, M., Al-Qodah, Z., Alananbeh, K., Bouqellah, N., Assirey, E., Bani-Melhem, K., 2014. COD reduction of baker's yeast wastewater using batch electrocoagulation. *Environ. Eng. Manage. J.* 13, 3153–3160.
- Al-Shannag, M., Al-Qodah, Z., Bani-Melhem, K., Qtaishat, M.R., Alkasrawi, M., 2015. Heavy metal ions removal from metal plating wastewater using electrocoagulation: kinetic study and process performance. *Chem. Eng. J.* 260, 749–756.
- Bautitz, I.R., Nogueira, R.F.P., 2007. Degradation of tetracycline by photo-Fenton process –solar irradiation and matrix effects. *J. Photochem. Photobiol. A* 187, 33–39.
- Bratby, J., 2006. Coagulation and Flocculation in Water and Wastewater Treatment, second ed. IWA Publishing, London.
- Carrier, X., Marceau, E., Lambert, J.F., Che, M., 2007. Transformations of γ -alumina in aqueous suspensions: 1. Alumina chemical weathering studied as a function of pH. *J. Colloid Interface Sci.* 308, 429–437.
- Chang, P.H., Jean, J.S., Jiang, W.T., Li, Z., 2009. Mechanism of tetracycline sorption on rectorite. *Colloids Surf. A: Physicochem. Eng. Asp.* 339, 94–99.
- Chen, X., Chen, G., Yue, P.L., 2000. Separation of pollutants from restaurant wastewater by electrocoagulation. *Sep. Purif. Technol.* 19, 65–76.
- Choi, K.J., Kima, S.G., Kim, S.H., 2008. Removal of antibiotics by coagulation and granular activated carbon filtration. *J. Hazard. Mater.* 151 (1), 38–43.
- Chutia, P., Kato, S., KojimaT, SatokawaS., 2009. Arsenic adsorption from aqueous solution on synthetic zeolites. *J. Hazard. Mater.* 162, 440–447.
- Drouiche, N., Aoudj, S., Hecini, M., Ghaffour, N., Lounici, H., Mameri, N., 2009. Study on the treatment of photovoltaic

Electro-coagulation coupled electro-flotation process

- wastewater using electro-coagulation fluoride removal with aluminum electrodes characteristics of productions. *J. Hazard. Mater.* 169, 65–69.
- Dubinin, M.M., Radushkevich, L.V., 1947. Equation of the characteristic curve of activated charcoal. *Chem. Zent.* 1 (1), 875.
- Emamjomeh, M.M., Sivakumar, M., 2009. Review of pollutants removed by electrocoagulation and electrocoagulation/flotation processes. *J. Environ. Manage.* 90 (5), 1663–1679.
- Ezechi, E.H., Isa, M.H., Kutty, S.R.M., Yaqub, A., 2014. Boron removal from produced water using electrocoagulation. *Process Saf. Environ. Prot.* 92, 509–514.
- Figueroa, R.A., Leonard, A., MacKay, A.A., 2004. Modeling tetracycline antibiotic sorption on clay. *Environ. Sci. Technol.* 38, 476–483.
- Fukui, Y., Yuu, S., 1985. Removal of colloidal particles in electroflootation. *AIChE J.* 31, 201–208.
- Gao, P., Chen, X., Shen, F., Chen, G., 2005. Removal of chromium (VI) from wastewater by combined electrocoagulation–electroflootation without a filter. *Sep. Purif. Technol.* 43, 117–123.
- Ge, J., Qu, J., Lei, P., Liu, H., 2004. New bipolar electrocoagulation–electroflootation process for the treatment of laundry wastewater. *Sep. Purif. Technol.* 36, 33–39.
- Ghernaout, D., Ghernaout, B., Saiba, A., Boucherit, A., Kellil, A., 2009. Removal of humic acids by continuous electromagnetic treatment followed by electrocoagulation in batch using aluminum electrodes. *Desalination* 239, 295–308.
- Ghosh, D., Medhi, C.R., Purkait, M.K., 2008a. Treatment of fluoride containing drinking water by electrocoagulation using monopolar and bipolar electrode connections. *Chemosphere* 73, 1393–1400.
- Ghosh, D., Solanki, H., Purkait, M.K., 2008b. Removal of Fe(II) from tap water by electrocoagulation technique. *J. Hazard. Mater.* 155, 135–143.
- Glembotskii, V.A., Mamakov, A.A., Ramanov, A.M., Nenno, V.E., 1975. In: Proceedings of the 11th International Mineral Processing Congress, Cagliari, Italy, pp. 562–581.
- Ho, Y.S., 2006. Review of second order models for adsorption systems. *J. Hazard. Mater.* B136, 681–689.
- Ho, Y.S., Wase, D.A.J., Forster, C.F., 1996. Kinetic studies of competitive heavy metal adsorption by sphagnum moss peat. *Environ. Technol.* 17, 71–77.
- Holt, P.K., Barton, G.W., Mitchell, C.A., 2005. The future for electrocoagulation as a localized water treatment technology. *Chemosphere* 59, 355–367.
- Isa, M.H., Ezechi, E.H., Ahmed, Z., Magram, S.F., Kutty, S.R.M., 2014. Boron removal by electrocoagulation and recovery. *Water. Res.* 51, 113–123.
- Janpoor, F., Torabian, A., Khatibikamal, V., 2011. Treatment of laundry wastewater by electrocoagulation. *J. Chem. Technol. Biotechnol.* 86, 1113–1120.
- Ji, L., Chen, W., Duan, L., Zhu, D., 2009. Mechanisms for strong adsorption of tetracycline to carbon nano tubes: a comparative study using activated carbon and graphite as adsorbents. *Environ. Sci. Technol.* 43, 2322–2327.
- Juang, R.S., Chen, M.L., 1997. Application of the Elovich equation to the kinetics of metal sorption with solvent impregnated resins. *Ind. Eng. Chem. Res.* 36, 813–820.
- Kamaraj, R., Vasudevan, S., 2015. Evaluation of electrocoagulation process for the removal of strontium and cesium from aqueous solution. *Chem. Eng. Res. Des.* 93, 522–530.
- Kamaraj, R., Ganeshan, P., Lakshmi, J., Vasudevan, S., 2013. Removal of copper from water by electro-coagulation process – effect of alternating current (AC) and direct current (DC). *Environ. Sci. Pollut. Res.* 20, 399–412.
- Kashefialas, M., Khosravi, M., Marandi, R., Seyyedi, K., 2006. Treatment of dye solution containing colored index acid yellow 36 by electrocoagulation using iron electrodes. *Int. J. Environ. Sci. Technol.* 2, 365–371.
- Khan, M.H., Bae, H., Jung, J.Y., 2010. Tetracycline degradation by ozonation in the aqueous phase: proposed degradation intermediates and pathway. *J. Hazard. Mater.* 181, 659–665.
- Khatibikamal, V., Torabian, A., Janpoor, F., Hoshayaripour, G.A., 2010. Fluoride removal from industrial wastewater using electrocoagulation and its adsorption kinetics. *J. Hazard. Mater.* 179, 276–280.
- KobyaM, Hiz.H., SenturkE, Aydiner.C., Demirbas, E., 2006. Treatment of potato chips manufacturing wastewater by electrocoagulation. *Desalination* 190, 201–211.
- Kotti, M., Dammak, N., Ksentini, I., Ben Mansour, L., 2009. Effects of impurities on oxygen transfer rate in the electroflootation process. *Indian J. Chem. Technol.* 16, 513–518.
- Kumar, P.R., Chaudhari, S., Khilar, K.C., Mahajan, S.P., 2004. Removal of arsenic from water by electrocoagulation. *Chemosphere* 55, 1245–1252.
- Lagergren, S., 1898. About the theory of so-called adsorption of soluble substances. *Handlingar* 24 (4), 1–39.
- Lakshmi, J., Sozhan, G., Vasudevan, S., 2013. Recovery of hydrogen and removal of nitrate from water by electrocoagulation process. *Environ. Sci. Pollut. Res.* 20, 2184–2192.
- Larue, O., Vorobiev, E., Durand, C.V.B., 2003. Electrocoagulation and coagulation by iron of latex particles in aqueous suspensions. *Sep. Purif. Technol.* 31, 177–192.
- Lin, S.H., Peng, C.F., 1996. Continuous treatment of textile wastewater by combined coagulation, electrochemical oxidation and activated sludge. *Water Res.* 30, 587–592.
- Liu, Y., Gan, X., Zhou, B., Xiong, B., Li, J., Dong, C., Bai, J., Cai, W., 2009. Photoelectrocatalytic degradation of tetracycline by highly effective TiO₂ nanopore arrays electrode. *J. Hazard. Mater.* 171, 678–683.
- Malakootian, M., Mansoorian, H.J., Moosazadeh, M., 2010. Performance evaluation of electrocoagulation process using iron-rod electrodes for removing hardness from drinking water. *Desalination* 255, 67–71.
- Mansour, S.E., Hasieb, I.H., Khalaf, H.A., 2012. Removal of cobalt from drinking water by alternating current electrocoagulation technique. *J. Appl. Sci.* 12 (8), 787–792.
- Merzouk, B., Gourich, B., Sekki, A., Madani, K., Vial, Ch., Barkaoui, M., 2009. Studies on the decolorization of textile dye wastewater by continuous electrocoagulation process. *Chem. Eng. J.* 149, 207–214.
- Nandi, B.K., Patel, S., 2014. Removal of brilliant green from aqueous solution by electrocoagulation using aluminum electrodes: experimental, kinetics, and modeling. *Sep. Sci. Technol.* 49 (4), 601–612.
- O'Connor, S., Aga, D.S., 2007. Analysis of tetracycline antibiotics in soil: advances in extraction, clean-up, and quantification. *TrAC Trend. Anal. Chem.* 26, 456–465.
- Okuda, T., Kobayashi, Y., Nagao, R., Yamashita, N., Tanaka, H., Tanaka, S., Fujii, S., Konishi, C., Houwa, I., 2008. Removal efficiency of 66 pharmaceuticals during wastewater treatment process in Japan. *Water Sci. Technol.* 57 (1), 65–71.
- Onyango, M.S., Kojima, Y., Aoyi, O., Bernardo, E.C., Matsuda, H., 2004. Adsorption equilibrium modeling and solution chemistry dependence of fluoride removal from water by trivalent-cation-exchanged zeolite F-9. *J. Colloid Interface Sci.* 279, 341–350.
- Ouaissa, Y.A., Chabani, M., Amrane, A., Bensmaili, A., 2014. Removal of tetracycline by electro-coagulation: kinetic and isotherm modeling through adsorption. *J. Environ. Chem. Eng.* 2, 177–184.
- Reyes, C., Fernandez, J., Freer, J., Mondaca, M.A., Zaror, C., Malato, S., Mansilla, H.D., 2006. Degradation and inactivation of tetracycline by TiO₂ photocatalysis. *J. Photochem. Photobiol. A: Chem.* 184, 141–146.
- Safety Data Sheet, 2014. According to 1907/2006/EC, Article 31, Version 2, Section 6, pp. 1–7.
- Swain, S.K., Dey, R.K., Islam, M., Patel, R.K., Jha, U., Patnaik, T., Airol迪, C., 2009. Removal of fluoride from aqueous solution using

- aluminum-impregnated chitosan biopolymer. *Sep. Sci. Technol.* 44, 2096–2116.
- Tsai, W.H., Huang, T.C., Chen, H.H., Huang, J.J., Hsue, M.H., Chuang, H.Y., Wu, Y.W., 2010. Determination of tetracyclines in surface water and milk by the magnesium hydroxide coprecipitation method. *J. Chromatogr. A* 1217, 415–418.
- United States Pharmacopeia (USP) DI, 1997. Drug Information for the Health Care Professional, 17th ed. United States Pharmacopeial Convention Inc., Rockville (MD).
- Vasudevan, S., Lakshmi, J., Sozhan, G., 2013. Electrochemically assisted coagulation for the removal of boron from water using zinc anode. *Desalination* 310, 122–129.
- Wan, Y., Bao, Y., Zhou, Q.X., 2010. Simultaneous adsorption and desorption of cadmium and tetracycline on cinnamon soil. *Chemosphere* 80, 807–812.
- Wang, Y.J., Jia, D.A., Sun, R.J., Zhu, H.W., Zhou, A.M., 2008. Adsorption and co-sorption of tetracycline and copper(II) on Montmorillonite as affected by solution pH. *Environ. Sci. Technol.* 42, 3254–3259.
- Weber, W.J., Morris, J.C., 1963. Kinetics of adsorption on carbon from solution. *J. Sanitary Eng. Div. Proceed. Am. Soc. Civil Eng.* 89, 31–59.
- Yavuz, Y., Öcal, E., Koparal, A.S., Öğütveren, Ü.B., 2011. Treatment of dairy industry wastewater by EC and EF processes using hybrid Fe–Al plate electrodes. *J. Chem. Technol. Biotechnol.* 86, 964–969.
- Zaroual, Z., Azzi, M., Saib, N., Chainet, E., 2006. Contribution to the study of electrocoagulation mechanism in basic textile effluent. *J. Hazard. Mater. B* 131, 73–78.
- Zhang, Z., Grover, D.P., Zhou, J.L., 2009. Monitoring pharmaceutical residues in sewage effluents. In: Ahuja, S. (Ed.), *Handbook of Water Purity and Quality*, Academic Press – Elsevier, Amsterdam, pp. 315–342.
- Zhang, Z., Sun, K., Gao, B., Zhang, G., Liu, X., Zhao, Y., 2011. Adsorption of tetracycline on soil and sediment: effects of pH and the presence of Cu (II). *J. Hazard. Mater.* 190, 856–862.
- Zhou, Y., Liang, Z., Wang, Y., 2008. Decolorization and COD removal of secondary yeast wastewater effluents by coagulation using aluminum sulfate. *Desalination* 225, 301–311.